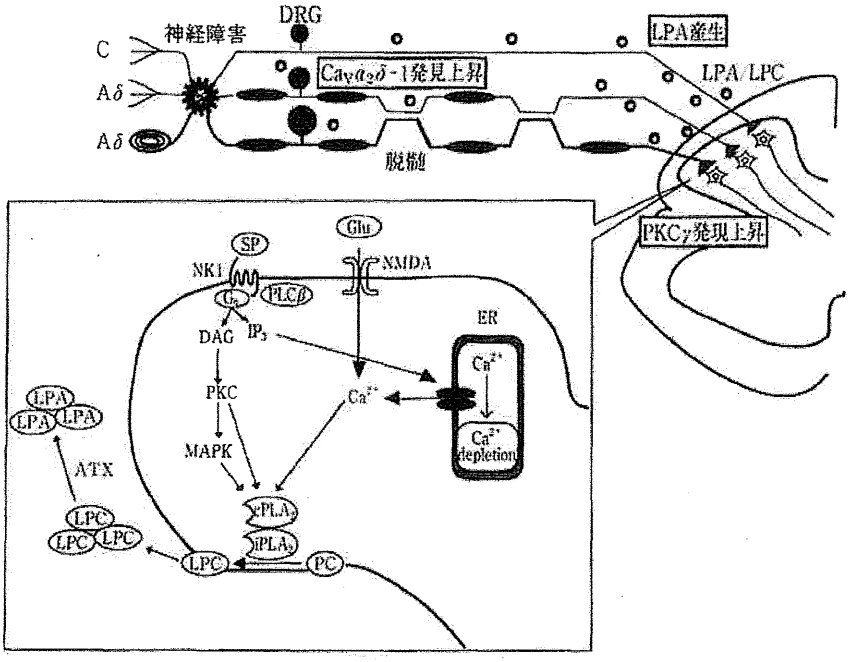

図　神経因性疼痛原因分子LPAのフィードフォワード性産生制御機構

ンビナントATXを添加した条件下で疼痛刺激に相当するカプサイシン刺激や脊髄疼痛伝達物質サブスタンスPやグルタミン酸刺激を行い，LPA産生の測定を行った。

興味あることに，LPC産生(LPAに変換されるが)はカプサイシン刺激で観察されるが，サブスタンスPとグルタミン酸のいずれか片方では観察されず，同時刺激を必要とした。このことは，末梢神経障害による極めて強い刺激を受けた一次知覚神経が，過剰な興奮または複数の異なる線維の刺激を脊髄後角に伝達することでLPAの産生を誘導するということ，すなわち慢性疼痛時のフィードフォワード性LPA産生制御機構の存在を示唆している。これまでに，LPA_1ノックアウトでは坐骨神経部分結紮やLPCの脊髄くも膜下腔内投与による神経障害性疼痛様のアロディニアと痛覚過敏応答は完全に消失するが，ATXヘテロノックアウトマウスにおいては神経損傷で誘発された神経因性疼痛の約50%の回復を示したことを報告している。LPA_1欠損マウスにおける平常時の疼痛閾値は対照群と変化がなく，恒常的なLPA産生は期待されないことから，通常の痛み刺激ではなく，神経因性疼痛を誘発するに要する強度の痛み刺激がLPA産生に必要であることが証明された。

*

一般に，急性の痛みは生体に与えられた侵害情報に対する警告としての機能を有するが，神経因性疼痛のように過剰で持続的な痛みが難治化すると患者のQOLを低下させ，その原因疾患に対する治療をますます困難なものにするため，迅速かつ適切なペインコントロールが不可欠である。末梢神経障害はそのレベルに留まらず，脊髄そして脳へと上位の神経機能の変調を引き起こし，そのメカニズムを複雑化させる。現在，筆者らは，末梢や脊髄レベルに留まらず上位脳におけるLPAの関与とその産生メカニズムを解明すべく研究を続けている。

文　献

1) Aoki J et al : *Biochim Biophys Acta* **1781** : 513-518, 2008
2) Inoue M et al : *Nature Med* **10** : 712-718, 2004
3) Ueda H : *Pharmacol Ther* **109** : 57-77, 2006
4) Ueda H : *Mol Pain* **4** : 11, 2008
5) Inoue M et al : *J Neurochem* **107** : 1556-1565, 2008

神経障害性疼痛を担うフィードフォワード増幅機構

植田弘師　内田仁司
長崎大学大学院医歯薬学総合研究科分子薬理学分野

要　旨
神経損傷により誘導される慢性疼痛は，抗炎症薬やモルヒネによって除痛されにくいことから難治性神経障害性疼痛と呼ばれている．筆者らは近年，神経損傷後，長期に認められる痛覚過敏とアロディニア現象を誘導する初発因子として，脂質メディエーターであるリゾホスファチジン酸を同定した．この分子は，強度の侵害刺激に応じて産生され，神経障害性疼痛の分子基盤となる疼痛関連分子の発現変調や脱髄現象を誘発する．さらにこの分子はグリア細胞を活性化し，これらがフィードフォワード増幅機構として痛みの慢性化につながる可能性が出てきた．
(ペインクリニック 30：1539-1544，2009)
キーワード：リゾホスファチジン酸，神経障害性疼痛，フィードフォワード機構

はじめに

神経損傷に起因する慢性疼痛（神経障害性疼痛）は，抗炎症薬やモルヒネ等の薬物に対して抵抗性を示し，有効な治療手段の確立されていない難治性疾患である．こうした慢性疼痛の多くは，その痛み伝達の仕組みが急性の痛みとは大きく異なることがその原因であるとされる．そのため，急性痛では著明な効果を示すモルヒネ鎮痛効果が減弱するという現象がみられる．1988年，BennettとXieによる部分的神経損傷モデルの報告[1]以降，多くの神経障害性疼痛モデルが開発され[2]，その分子機構は一次知覚神経と脊髄での可塑的機能変調として説明できるようになった[3]．これらに共通することは，いずれの場合も知覚神経の全結紮ではなく，部分的な損傷に基づくことであった．このことは，損傷を受けた神経そのものが症状を反映するのではなく，損傷の結果生ずる新たな液性因子が，知覚入力の可塑的再編成を誘発することを示唆するものである．筆者らは，2004年この神経障害性疼痛を誘発する因子がリゾホスファチジン酸（lysophosphatidic acid：LPA）であることを突き止めることに成功した[4]．本稿では，LPA誘発性神経障害性疼痛の分子基盤である，疼痛関連分子の発現変調，脱髄現象およびグリア細胞活性化を介したフィードフォワード増幅機構について概説する．さらに，脊髄におけるLPA産生機構について最近の知見を紹介する．

1．LPAによるフィードフォワード機構を介した神経障害性疼痛の誘導

LPAはグリセロール骨格にリン酸基と脂肪酸が1つずつ結合したリン脂質であり，細胞増殖，細胞運動，血小板凝集，平滑筋収縮など多彩な生理活性を有しており，がんや動脈硬化な

〈Review〉
Feed-forward amplifier system underlying neuropathic pain
Hiroshi Ueda, et al
Division of Molecular Pharmacology and Neuroscience, Nagasaki University Graduate School of Biomedical Sciences

どに関与することが知られる[5]．LPAの作用は各種のG蛋白質（$G_{q/11/11}$，$G_{12/13}$，$G_{i/o}$）と共役する7回膜貫通型受容体（$LPA_{1\text{-}5}$，P2Y5，P2Y10，GPR87）を介することが想定されている[6]．$G_{i/o}$蛋白質を介したPI_3キナーゼ-Akt経路の活性化に伴い生存効果を示す一方で，$G_{12/13}$蛋白質を介したRho-Rhoキナーゼ経路の活性化により細胞の形態的変化を誘導する．また，シュワン細胞やオリゴデンドロサイトに対してもその形態的変化を促し，ミエリンの形成に影響を与えることが報告されている[7,8]．ミエリン形成異常である脱髄現象は，多発性硬化症[9]やギランバレー症候群[10]などの難治性疾患において確認されており，同時にこれらの疾患は著しい知覚過敏現象を伴うことから，疼痛と密接に関連することが示唆されている．傷害時にはLPAが著明に産生されることが広く知られていることから，筆者らは，神経損傷性神経障害性疼痛におけるLPAの関与を想定した．LPAを脊髄くも膜下腔内に単回投与した時，驚くべきことに1～2日後に始まり，1週間以上も持続する神経障害性疼痛様の知覚過敏症状とアロディニア現象が認められた[4]．さらに，神経損傷性モデルと同様に，LPA投与により脊髄後根部位において著しい脱髄現象が観察された．この脱髄現象は知覚過敏症状およびアロディニア現象と時間経過が完全に一致しており，神経障害性疼痛における脱髄現象の関与を裏付けるものであった．最も重要な発見は，LPAおよび神経傷害による行動学的および形態学的な変調が，LPA_1受容体遺伝子欠損マウス，RhoA阻害薬であるボツリヌス毒素C3処置，Rhoキナーゼ阻害薬であるY-27632処置においてほぼ完全に消失した事実である．このことは，LPA_1受容体を介した$G_{12/13}$蛋白質およびRho-Rhoキナーゼの活性化が，神経障害性疼痛において重要な役割を果たすことを示唆している．以下に，最近の研究成果を踏まえて，LPAによるフィードフォワード増幅機構を介した神経障害性疼痛の分子基盤について述べる．

1）脱髄現象

LPAによる脱髄現象の分子基盤は，シュワン細胞におけるMBP（myelin basic protein）やPMP22（peripheral myelin protein 22）などのミエリン関連分子の発現低下である[4]．先に述べたように，神経損傷時におけるLPA_1受容体を介した脱髄現象は脊髄後根に特異的に生じる．一方，LPA_1受容体の発現は脊髄後根のみならず，脊髄神経および坐骨神経においても観察される．実際に，知覚線維の*ex vivo*培養実験[11]において，各部位におけるLPA感受性脱髄現象の有無を調べたところ，いずれの部位においても有意な脱髄現象が観察された．このことは，神経障害性疼痛時におけるLPAの産生部位が脊髄側に局所的に生じていることを示唆しており，LPA産生部位・産生機構を同定するために非常に興味深い．

神経障害性疼痛との関連において，脱髄現象は隣接する線維との間に電気的な混線（エファプス）を生じることで，侵害情報の拡散・過興奮が起こり，アロディニア現象を招くと考えられる．また，脱髄により神経の異常突起伸展（スプラウティング）が生じ，脊髄入力側末端においてのシナプス誤入力を招き，知覚異常に至ることも推測される．さらには，損傷後のシュワン細胞はサイトカインなどの液性因子を遊離し，一次知覚神経の遺伝子発現を変化させることも指摘されている[12]．したがって，LPAによる脱髄現象は，二次的に神経の可塑的機能変調を誘発し，フィードフォワード増幅機構として機能することが考えられる（図1）．また最近，一次知覚神経に加えて，LPAは三叉神経の脱髄現象を介してアロディニアを誘発することが報告された[13]．この現象においてもLPA受容体を介したRhoキナーゼ活性化の関与が見い出されている．

2）疼痛関連分子の遺伝子発現変調

われわれは，知覚線維特異的侵害受容評価法を用いて，神経障害性疼痛の分子基盤として，無髄C線維の機能消失と有髄A線維の機能亢進を見い出している[2]．さらに，LPA_1受容体

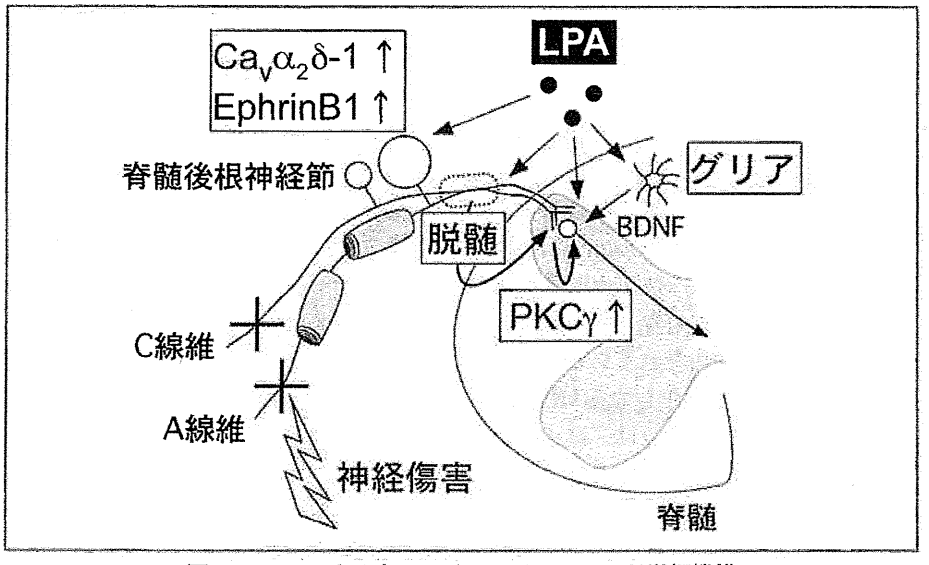

図1　LPAによる痛みのフィードフォワード増幅機構
脊髄において産生されたLPAは，複数の経路を介して痛みの増幅機構を誘発する．一つ目は疼痛関連分子の発現変調であり，一次知覚神経における $Ca_v\alpha_2\delta$-1 やephrinB1の発現増加，脊髄二次神経におけるPKCγの発現増加を介して脊髄疼痛伝達を増強させる．二つ目は，脊髄後根におけるミエリン関連蛋白質の発現低下を介した脱髄現象である．脱髄は，神経線維間の混線や脊髄後角における知覚神経の誤入力を介して，異常痛を誘発する．三つ目はミクログリア活性化であり，BDNFなどの液性因子遊離を介して脊髄疼痛伝達を増強させる

シグナリングがその分子基盤であることも明らかにした[14]．具体的に述べると，LPAは脊髄後角において，無髄C線維の神経伝達物質の一つであるサブスタンスP（substance P：SP）免疫活性を著明に低下させた[15]．その分子機構については，後根神経節（dorsal root ganglion：DRG）における著明なSP発現低下が認められなかったことから，LPAによる無髄C線維の神経退縮の可能性が考えられる．一方，LPAは有髄A線維のDRGにおける，神経伝達物質遊離に関与するカルシウムチャネル $\alpha_2\delta$-1サブユニット（$Ca_v\alpha_2\delta$-1）の新規発現を誘発させた[4]．さらに最近，遺伝子発現の網羅的解析結果から，DRGにおいて LPA_1 受容体シグナリングにより高度に制御される遺伝子として，ephrinB1を初めとするグルタミン酸－NMDA（*N*-methyl-D-aspartate）受容体関連遺伝子群を新規同定した[16]．前シナプス膜一回貫通型のephrinB1は後シナプス膜のEphB受容体と相互作用し，リン酸化によるNMDA受容体活性化を誘発することが知られる[17]．われわれは，機能解析を通じて，LPA誘発性のA線維機能亢進および神経障害性疼痛においてephrinB1が重要な役割を果たすことを明らかにした[16]．また最近，この結果を支持するように，神経障害性疼痛における脊髄後角のephrinB-EphB受容体システムの関与が報告されている[18]．さらに，LPAは脊髄後角におけるプロテインキナーゼCγ（protein kinase Cγ：PKCγ）の発現増加を誘発した[4]．PKCγはNMDA受容体活性化の下流に働くことが知られ，また，PKCγ遺伝子欠損マウスでは神経障害性疼痛が消失することが報告されている[19]．以上の知見は，LPAが遺伝子発現変調を介したフィードフォワード増幅機構により，A線維を介するNMDA受容体応答を増強させ，神経障害性疼痛を誘発することを強く示唆している（図1）．

3）グリア細胞の活性化

最近，神経障害性疼痛における神経－グリア相関が重要視されている[20]．特に脊髄ミクログリアは，神経栄養因子やサイトカイン遊離を介して，神経障害性疼痛の分子基盤となる神経の可塑的機能変調をする[20]．代表的な神経栄養因子である脳由来神経栄養因子（brain-derived neurotrophic factor：BDNF）はTrkB受容体に作用し，少なくとも2つの経路により脊髄疼痛伝達を増強することが報告されている．1つは，PKCによるリン酸化を介したNMDA受容体活性化である[21,22]．もう1つは，陰イオンポンプ（K^+-Cl^- cotransporter：KCC2）の発現低下を介して細胞内Cl^-濃度を上昇させ，その結果として神経伝達物質GABA（γ-aminobutyric acid）の働きを抑制性から興奮性に変換するという機構である[23,24]．われわれは，LPAが培養ミクログリアに作用し，ATP遊離を介してBDNF発現を誘発することを見い出している[25]．このことは，LPAが脊髄ミクログリアを介したフィードフォワード機構を駆動させることを示唆している（図1）．具体的には，神経損傷初期における脊髄ミクログリアの活性化が神経障害性疼痛の形成に関与することが報告されており[26]，この機構におけるLPAの関与が考えられる．

2．神経傷害時におけるLPA生合成機構

LPA産生には，少なくとも2つの経路が存在している．1つはジアシルグリセロールから産生されたホスファチジン酸がLPAに変換される経路であり，もう1つはホスファチジルコリンから産生されたリゾホスファチジルコリン（lysophosphatidylcholine：LPC）がリゾホスホリパーゼD/オートタキシン（autotaxin：ATX）によりLPAに変換される経路である[5]．このうち，体液中，特に血液中のLPA産生には主に後者の経路が関与する．これまでにわれわれは，ATXヘテロ変異マウスにおいてLPA誘発性の神経障害性疼痛が顕著に減弱すること[27]，およびLPC投与がLPA_1受容体依存的な疼痛過敏とアロディニアを誘発することを見い出している[28]．また，LPA_1受容体遺伝子欠損マウスおよびATXヘテロ変異マウスにおいて，非傷害時の疼痛閾値は野生型マウスと変わりなく，LPA産生およびその下流の機構は神経傷害特異的に生じることが示唆された．

そこで，LPA_1受容体発現細胞を用いたバイオアッセイ法を確立し，薬物処理後の脊髄切片上清に含まれるLPAを定量解析した．まず，一次知覚神経に対する強度の侵害刺激がLPA産生を誘発すると想定し，脊髄切片をカプサイシン刺激したところ著明なLPA産生が認められた．次に，SPやNMDAを始めとする種々の神経伝達物質を用いて解析したところ，単独刺激ではLPA産生は認められず，SPとNMDAの同時刺激においてのみLPA産生が観察された[29]．さらに，各種阻害薬を用いた解析から，脊髄におけるLPA産生機構には，NK1（neurokinin 1）受容体とNMDA受容体の同時刺激によるカルシウム依存性のホスホリパーゼA_2（cytosolic phospholipase A_2：$cPLA_2$）および非依存性の$iPLA_2$（Ca^{2+}-independent PLA_2）の活性化が関与することを明らかにした（図2）．神経栄養因子やサイトカインにおいても，MAPK（mitogen-activated protein kinase）を介した$cPLA_2$活性化により，LPA産生に関与することが考えられる．

さらに最近，神経損傷後におけるLPA産生およびその作用の臨界期について，短時間作用型LPA_1受容体拮抗薬であるKi-16425を用いた薬理学的アプローチで解析を行った[30]．その結果，損傷3時間後のKi-16425投与は，損傷7日後の神経障害性疼痛，DRGにおける$Ca_v\alpha_2\delta$-1発現増加，脊髄後角におけるSP発現低下をすべて抑制した．しかしながら，損傷6時間後のKi-16425投与は効果を示さなかった．更なる詳細な解析結果から，神経損傷2～3時間においてLPA産生およびLPA_1受容体シグナリングが駆動することが明らかになった．フィードフォワード増幅機構により増強した疼痛伝達が，更なるLPA産生を誘発するという可能性も考えられる．この点に関しては，今後

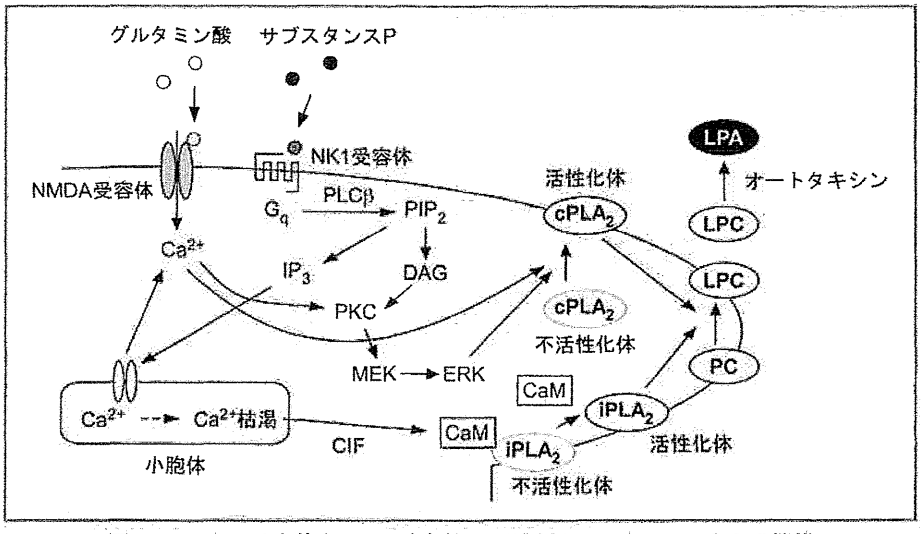

図2　NMDA受容体とNK1受容体の同時刺激によるLPA生合成機構
グルタミン酸とサブスタンスPによるNMDA受容体とNK1受容体の同時刺激は，ジアシルグリセロール（diacylglycerol：DAG）あるいはイノシトール三リン酸（inositol (1,4,5) triphosphate：IP_3）シグナリングを介して，PKCおよびmitogen-activated proteinkinase kinase（MEK）/extracellular-regulated kinase（ERK）の活性化あるいは細胞内カルシウム濃度上昇を引き起こす．これらの経路は$cPLA_2$および$iPLA_2$の活性化を介してLPC産生を誘発する．遊離したLPCは，オートタキシンによりLPAに変換される．
Phospholipase Cβ（PLCβ），phosphatidylinositol 4,5-biphosphate（PIP_2），phosphatidylcholine（PC），calmodulin（CaM），calcium influx factor（CIF）

の課題である．

おわりに

一般に，急性の痛みは生体に与えられた侵害情報に対する警告としての機能を有するが，神経障害性疼痛のように過剰で持続的な痛みが難治化すると患者の生活の質（quality of life：QOL）を低下させ，その原因疾患に対する治療をますます困難なものにするため，迅速かつ適切なペインコントロールが不可欠である．末梢神経傷害はそのレベルに留まらず，脊髄そして脳へと上位の神経機能の変調を引き起こし，そのメカニズムを複雑化させる．現在，筆者らは末梢や脊髄レベルに留まらず上位脳におけるLPAの関与とその産生メカニズムを解明すべく研究を続けている．

文　献

1) Bennett GJ, Xie YK：A peripheral mononeuropathy in rat that produces disorders of pain sensation like those seen in man. Pain 33：87-107, 1988
2) Ueda H：Molecular mechanisms of neuropathic pain-phenotypic switch and initiation mechanisms. Pharmacol Ther 109：57-77, 2006
3) Costigan M, Scholz J, Woolf CJ：Neuropathic pain：A maladaptive response of the nervous system to damage. Annu Rev Neurosci 32：1-32, 2009
4) Inoue M, Rashid MH, Fujita R, et al：Initiation of neuropathic pain requires lysophosphatidic acid receptor signaling. Nat Med 10：712-718, 2004
5) Aoki J, Inoue A, Okudaira S：Two pathways for lysophosphatidic acid production. Biochim Biophys Acta 1781：513-518, 2008
6) Noguchi K, Herr D, Mutoh T, et al：Lysophosphatidic acid (LPA) and its receptors. Curr Opin Pharmacol 9：15-23, 2009
7) Ye X, Fukushima N, Kingsbury MA, et al：Lysophosphatidic acid in neural signaling. Neuroreport 13：2169-2175, 2002
8) Saba JD：Lysophospholipids in development：Miles apart and edging in. J Cell Biochem

92 : 967-992, 2004
9) Neuhaus O, Archelos JJ, Hartung HP: Immunomodulation in multiple sclerosis: from immunosuppression to neuroprotection. Trends Pharmacol Sci 24 : 131-138, 2003
10) Ang CW, Jacobs BC, Laman JD: The Guillain-Barre syndrome: a true case of molecular mimicry. Trends Immunol 25 : 61-66, 2004
11) Fujita R, Kiguchi N, Ueda H: LPA-mediated demyelination in *ex vivo* culture of dorsal root. Neurochem Int 50 : 351-355, 2007
12) Thacker MA, Clark AK, Marchand F, et al: Pathophysiology of peripheral neuropathic pain: immune cells and molecules. Anesth Analg 105 : 838-847, 2007
13) Ahn DK, Lee SY, Han SR, et al: Intratrigeminal ganglionic injection of LPA causes neuropathic pain-like behavior and demyelination in rats. Pain 2009 [Epub ahead of print]
14) Ueda H: Peripheral mechanisms of neuropathic pain-involvement of lysophosphatidic acid receptor-mediated demyelination. Mol Pain 4 : 11, 2008
15) Inoue M, Yamaguchi A, Kawakami M, et al: Loss of spinal substance P pain transmission under the condition of LPA1 receptor-mediated neuropathic pain. Mol Pain 2 : 25, 2006
16) Uchida H, Matsumoto M, Ueda H: Profiling of BoNT/C3-reversible gene expression induced by lysophosphatidic acid: ephrinB1 gene upregulation underlying neuropathic hyperalgesia and allodynia. Neurochem Int 54 : 215-221, 2009
17) Calo L, Cinque C, Patane M, et al: Interaction between ephrins/Eph receptors and excitatory amino acid receptors: possible relevance in the regulation of synaptic plasticity and in the pathophysiology of neuronal degeneration. J Neurochem 98 : 1-10, 2006
18) Song XJ, Zheng JH, Cao JL, et al: EphrinB-EphB receptor signaling contributes to neuropathic pain by regulating neural excitability and spinal synaptic plasticity in rats. Pain 139 : 168-180, 2008
19) Malmberg AB, Chen C, Tonegawa S, et al: Preserved acute pain and reduced neuropathic pain in mice lacking PKCgamma. Science 278 : 279-283, 1997
20) Scholz J, Woolf CJ: The neuropathic pain triad: neurons, immune cells and glia. Nat Neurosci 10 : 1361-1368, 2007
21) Kerr BJ, Bradbury EJ, Bennett DL, et al: Brain-derived neurotrophic factor modulates nociceptive sensory inputs and NMDA-evoked responses in the rat spinal cord. J Neurosci 19 : 5138-5148, 1999
22) Slack SE, Pezet S, McMahon SB, et al: Brain-derived neurotrophic factor induces NMDA receptor subunit one phosphorylation via ERK and PKC in the rat spinal cord. Eur J Neurosci 20 : 1769-1778, 2004
23) Coull JA, Boudreau D, Bachand K, et al: Trans-synaptic shift in anion gradient in spinal lamina I neurons as a mechanism of neuropathic pain. Nature 424 : 938-942, 2003
24) Coull JA, Beggs S, Boudreau D, et al: BDNF from microglia causes the shift in neuronal anion gradient underlying neuropathic pain. Nature 438 : 1017-1021, 2005
25) Fujita R, Ma Y, Ueda H: Lysophosphatidic acid-induced membrane ruffling and brain-derived neurotrophic factor gene expression are mediated by ATP release in primary microglia. J Neurochem 107 : 152-160, 2008
26) Raghavendra V, Tanga F, DeLeo JA: Inhibition of microglial activation attenuates the development but not existing hypersensitivity in a rat model of neuropathy. J Pharmacol Exp Ther 306 : 624-630, 2003
27) Inoue M, Ma L, Aoki J, et al: Autotaxin, a synthetic enzyme of lysophosphatidic acid (LPA), mediates the induction of nerve-injured neuropathic pain. Mol Pain 4 : 6, 2008
28) Inoue M, Xie W, Matsushita Y, et al: Lysophosphatidylcholine induces neuropathic pain through an action of autotaxin to generate lysophosphatidic acid. Neuroscience 152 : 296-298, 2008
29) Inoue M, Ma L, Aoki J, et al: Simultaneous stimulation of spinal NK1 and NMDA receptors produces LPC which undergoes ATX-mediated conversion to LPA, an initiator of neuropathic pain. J Neurochem 107 : 1556-1565, 2008
30) Ma L, Matsumoto M, Xie W, et al: Evidence for lysophosphatidic acid 1 receptor signaling in the early phase of neuropathic pain mechanisms in experiments using Ki-16425, a lysophosphatidic acid 1 receptor antagonist. J Neurochem 109 : 603-610, 2009

※ ※ ※

Journal of Peptide Science

Synthetic pentapeptides inhibiting autophosphorylation of insulin receptor in a non-ATP-competitive mechanism

Journal:	*Journal of Peptide Science*
Manuscript ID:	PSC-08-0106.R1
Wiley - Manuscript type:	Research Article
Date Submitted by the Author:	27-Nov-2008
Complete List of Authors:	Kato, Masaki; Kyoto University, Graduate School of Pharmaceutical Sciences Abe, Mineo; Kyoto University, Graduate School of Pharmaceutical Sciences Kuroda, Yoshihiro; Himeji Dokkyo University, Faculty of Pharmaceutical Sciences Hirose, Munetaka; Fukui University, Faculty of Medicine Nakano, Minoru; Kyoto University, Graduate School of Pharmaceutical Sciences Handa, Tetsurou; Kyoto University, Graduate School of Pharmaceutical Sciences
Keywords:	insulin receptor, phosphorylation, autoinhibition, non-ATP-competitive, peptide inhibitor

Title page

Synthetic pentapeptides inhibiting autophosphorylation of insulin receptor in a non-ATP-competitive mechanism

Masaki Kato,[1] Mineo Abe,[1] Yoshihiro Kuroda,[2] Munetaka Hirose,[3] Minoru Nakano,[1] and Tetsurou Handa[1]

[1] Graduate School of Pharmaceutical Sciences, Kyoto University, Sakyo-ku, Kyoto 606-8501, Japan
[2] Faculty of Pharmaceutical Sciences, Himeji Dokkyo University, Himeji, Hyogo 670-8524, Japan
[3] Department of Anesthesiology and Reanimatology, Faculty of Medicine, Fukui University, Eiheiji-cho, Yoshida-gun, Fukui 910-1193, Japan

Correspondence to: Yoshihiro Kuroda, Faculty of Pharmaceutical Sciences, Himeji Dokkyo University, Himeji, Hyogo 670-8524, Japan; e-mail: yokuroda@himeji-du.ac.jp

Short Title: Inhibition of insulin receptor by small peptides

Keywords: insulin receptor, phosphorylation, autoinhibition, non-ATP-competitive, peptide inhibitor

Abbreviations: IR, insulin receptor; RTK, receptor tyrosine kinase; EGFR, epidermal growth factor receptor; EGF, epidermal growth factor; pY, phosphotyrosine; pTyr, phosphotyrosine

ABSTRACT

In an attempt to develop non-ATP-competitive inhibitors of the autophosphorylation of insulin receptor (IR), the effects of the synthetic peptides, Ac-DIY^{1158}ET-NH_2 and Ac-DY^{1162}Y^{1163}RK-NH_2, on the phosphorylation of IR were studied in vitro. The peptides were derived from the amino-acid sequence in the activation loop of IR. They inhibited the autophosphorylation of IR to 20.5 and 40.7%, respectively at 4000 μM. The Asp/Asn- and Glu/Gln-substituted peptides, Ac-NIYQT-NH_2 and Ac-NYYRK-NH_2, more potently inhibited the autophosphorylation than did the corresponding parent peptides. The inhibitory potencies of the substituted peptides were decreased with increasing concentrations of ATP, indicating that these peptides employ an ATP-competitive mechanism in inhibiting the autophosphorylation of IR. In contrast, those of the parent peptides were not affected. Mass spectrometry showed that the parent peptides were phosphorylated by IR, suggesting that they interact with the catalytic loop. Moreover, docking simulations predicted that the substituted peptides would interact with the ATP-binding region of IR, whereas their parent peptides would interact with the catalytic loop of IR. Thus, Ac-DIYET-NH_2 and Ac-DYYRK-NH_2 are expected to be non ATP-competitive inhibitors. These peptides could contribute to the development of a drug employing a novel mechanism.

INTRODUCTION

Receptor tyrosine kinases (RTKs) play an important role in the regulation of most fundamental cellular processes such as proliferation, differentiation, migration, and metabolism.[1–3] Uncontrolled and elevated RTK activity resulting from overexpression is associated with a range of human malignant tumors.[3,4] Inhibition of these receptors therefore represents a potent approach for the treatment of various cancers.

Insulin receptor (IR) is an $\alpha 2\beta 2$ heterotetrameric transmembrane protein possessing intrinsic tyrosine kinase activity.[5] Binding of insulin to the α-subunit elevates tyrosine-specific phosphotransferase activity, which leads to the autophosphorylation of specific tyrosine residues, called 'autophosphorylation sites', in the cytoplasmic β-subunit of IR. The autophosphorylation sites, which are mainly responsible for the activation of substrates, consist of three tyrosine residues (Tyr1158, Tyr1162, and Tyr1163) on the activation loop in the kinase domain.[6] The autophosphorylation sites recruit signaling proteins such as insulin receptor substrate-1, Shc, and Grb2. IR activates them, and then stimulates multiple intracellular signaling cascades such as the PI(3)K pathway, CAP/Cbl pathway, and Ras/MAPK pathway, which induce glucose metabolism, protein synthesis, and cell proliferation.[7,8]

The kinase activities of RTKs have unique regulation. In the inactive state, some domains of RTKs bind to their own kinase domains and kinase activities are suppressed.[9] Binding of an intrinsic ligand molecule to inactive RTK leads to conformational change of RTK, followed by activation of RTK and phosphorylation of substrates. The details of the autoinhibition mechanisms of several RTKs have been clarified. The C-terminal tails of Tie2 kinase,[10] PDGFR,[11] VEGFR-2,[12] and RON kinase[13] interact with their kinase domains and inhibit their own activities. On the other hand, the activity of Ephb2 receptor is regulated by its own juxtamembrane region.[14] The activation loop in the kinase domain of IR autoinhibits kinase activity by binding to its own catalytic region.[15–17] In an inactive state, the catalytic loop of IR (H^{1130}RDLAARN^{1137}), which plays a crucial role in phosphotransfer reactions, is hidden by the activation loop. Once three tyrosine residues in the activation loop (Tyr1158, Tyr1162, and Tyr1163) are phosphorylated, the activation loop dissociates from the catalytic loop with ligand-stimulated conformational change of the β-subunit. The catalytic loop exposed to solvent can phosphorylate the autophosphorylation sites (Tyr965, Tyr972, Tyr1158, Tyr1162, Tyr1163, Tyr1328, and Tyr1334) of another β-subunit in a *trans* manner and IR is activated.

Previously, we found that a pentapeptide, Ac-DIYET-NH_2, inhibits the autophosphorylation of IR.[18] The peptide includes the amino-acid sequence around an autophosphorylation site (Tyr1158) in the activation loop of IR (G^{1149}DFGMTRDIY^{1158}ETDY^{1162}Y^{1163}RKGGKGL^{1170}). We focused on the other autophosphorylation sites in the activation loop, i.e. Tyr1162 and Tyr1163, and synthesized a

peptide, Ac-DYYRK-NH_2, which consists of the amino-acid sequence around these autophosphorylation sites. In this study, we investigated the effects of Ac-DIYET-NH_2, Ac-DYYRK-NH_2, and their modified peptides on the autophosphorylation of IR. Moreover, inhibition mechanisms by the peptides, which were not proved in the previous study, are also investigated and discussed.

MATERIALS AND METHODS

Materials

Antiphosphotyrosine antibody 4G10 was obtained from Upstate Biotechnology (Lake Placid, NY). Purified IR from rat liver, purified epidermal growth factor receptor (EGFR) from human carcinoma A431 cells, insulin, and epidermal growth factor (EGF) were obtained from Sigma Chemical (St. Louis, MO). All Fmoc-L-amino acids were purchased from the Peptide Institute (Osaka, Japan), except Fmoc-L-Tyr{PO(OBzl)OH}-OH, which was from Watanabe Chemical Industries (Hiroshima, Japan).

Synthesis and purification of peptides

Peptides were synthesized automatically by the solid phase method using Fmoc chemistry on an ABI 433A Peptide Synthesizer (Applied Biosystems, Foster, CA). Their N-termini were acetylated (Ac-) and C-termini were amidated (-NH_2). After cleavage with TFA, the peptides were purified on a reverse phase C_{18} HPLC column (Waters, Milford, MA) using a gradient from 100% A, 0% B to 60% A, 40% B in 40 min, where A is 0.1% TFA in water and B is 0.1% TFA in acetonitrile. The peptides were characterized by mass spectrometry using a Sciex API III Mass Spectrometer (PerkinElmer Life and Analytical Sciences, Wellesley, MA) and Mariner-E Biospectrometry Workstation (PerSeptive Biosystems, Framingham, MA). Ac-DIYET-NH_2: *m/z* calculated 680.30 (monoisotope), 680.70 (average), found 681.5 ($[M+H]^+$); Ac-DYYRK-NH_2: *m/z* calculated 784.39 (monoisotope), 784.86 (average), found 785.5 ($[M+H]^+$); Ac-DIAET-NH_2: *m/z* calculated 588.28 (monoisotope), 588.61 (average), found 589.2 ($[M+H]^+$); Ac-DAARK-NH_2: *m/z* calculated 600.33 (monoisotope), 600.67 (average), found 601.2 ($[M+H]^+$); Ac-DIFET-NH_2: *m/z* calculated 664.31 (monoisotope), 664.70 (average), found 665.3 ($[M+H]^+$); Ac-DFFRK-NH_2: *m/z* calculated 752.40 (monoisotope), 752.86 (average), found 753.4 ($[M+H]^+$); Ac-DIpYET-NH_2: *m/z* calculated 760.27 (monoisotope), 760.68 (average), found 761.3 ($[M+H]^+$); Ac-DpYpYRK-NH_2: *m/z* calculated 944.32 (monoisotope), 944.82 (average), found 946.3 ($[M+H]^+$); Ac-NIYQT-NH_2:

m/z calculated 678.33 (monoisotope), 678.73 (average), found 679.5 ($[M+H]^+$); Ac-NYYRK-NH_2: *m/z* calculated 783.40 (monoisotope), 783.87 (average), found 784.5 ($[M+H]^+$).

In vitro phosphorylation of IR in the presence of synthetic peptides

Purified IR (4.1 μg/ml) was phosphorylated with or without 2.6 μg/ml insulin and synthetic peptides for 10 min at 37°C in 50 μl of incubation buffer, including 50 mM HEPES, pH 7.4, 125 mM NaCl, 1 mM EDTA, 10 mM $MgCl_2$, 5 mM $MnCl_2$, 5 mM dithiothreitol, 1 mM phenylmethylsulfonyl fluoride, and ATP. The concentration of ATP was 20 μM unless otherwise noted. After the reactions were stopped by the addition of Laemmli sample buffer and boiling for 5 min, IRs were separated by SDS-PAGE in 7.5% (v/v) acrylamide gels and transferred to a PVDF membrane (GE Healthcare Bio-Sciences, Piscataway, NJ). The membranes were blocked in 1% (w/v) BSA in tris buffered saline-0.1% Tween 20 at room temperature overnight, and then immunoblotted with antiphosphotyrosine antibody 4G10. The antigen-antibody complexes were visualized with Western blotting luminol reagent (Santa Cruz Biotechnology, Santa Cruz, CA). The bands were exposed to X-ray films (Fuji Photo Film, Tokyo, Japan) and images were analyzed by Scion Image 4.0.2 (Scion, Frederick, MD).

In vitro phosphorylation of EGFR in the presence of synthetic peptides

Purified EGFR (1.9 μg/ml) was phosphorylated with or without 10 μg/ml EGF and synthetic peptides for 10 min at 37°C in 50 μl of the incubation buffer including 20 μM ATP. After the reactions were stopped by the addition of Laemmli sample buffer and boiling for 5 min, EGFRs were separated by SDS-PAGE, followed by immunoblot analysis with antiphosphotyrosine antibody 4G10.

Statistical analysis

Experimental data were analyzed by one-way analysis of variance with Dunnett's post-hoc analysis. Statistical significance was established at $P<0.05$. All values are reported as the means ± standard deviations.

Studies on phosphorylation of synthetic peptides by mass spectrometry

Purified IR (41 μg/ml) was incubated for 30 min at 37°C with 2.6 μg/ml insulin, 20 μM ATP, 1 μM DIYET, 1 μM DYYRK, 1 μM NIYET, and 1 μM NYYRK. The reaction mixture was desalted

with the solid-phase extraction method using Discovery DSC-18 (Supelco, Bellefonte, PA). The eluent was 75% A, 25% B for DIYET, 80% A, 20% B for DYYRK, 70% A, 30% B for NIYQT, or 60% A, 40% B for NYYRK, where A is 0.1% TFA in water and B is 0.1% TFA in acetonitrile. The molecular masses of peptides in the sample solution were analyzed with a Sciex API III Mass Spectrometer and Mariner-E Biospectrometry Workstation.

System setup for docking simulations

The X-ray structure of the kinase domain of IR (IRK),[16] which is 303 amino acids long (Ser981–Lys1283) and bound with an ATP analogue and a peptide substrate, was from the RCSB Protein Data Bank.[19] The PDB ID is 1IR3. Coordinate files of the synthetic peptides, assuming an extended structure, were created using PyMOL v0.99 (DeLano Scientific LLC, South San Francisco, CA).[20] Each was manually placed at the substrate-binding site of IRK using the UCSF Chimera package (The Resource for Biocomputing, Visualization, and Informatics at the University of California, San Francisco, CA).[21] The direction of N- and C-termini of the peptide was the same as that of the peptide substrate. Charges of all atoms were assigned and added according to the all atom charge model of AMBER 94.[22] Hydrogen atoms were added with standard geometries.

Docking simulations – GRID Scoring Function

The prepared coordinate files for docking simulations were processed by the DOCK Suite of Programs 6.1: SPHGEN, GRID, DOCK, and other accessories (URL: http://dock.compbio.ucsf.edu/; University of California, San Francisco, CA).[23,24] A molecular surface was created for IRK using the DMS program (URL: http://www.cgl.ucsf.edu/Overview/software.html), and then used in SPHGEN to calculate spheres for docking.[25] Force field grids were calculated in GRID.[26] GRID scores are approximate interaction energies including van der Waals and electrostatic components:

$$\text{Score} = \sum_{i=1}^{\text{peptide}} \left(\sqrt{A_{ii}} \sum_{j=1}^{\text{IRK}} \frac{\sqrt{A_{jj}}}{r_{ij}^{12}} - \sqrt{B_{ii}} \sum_{j=1}^{\text{IRK}} \frac{\sqrt{B_{jj}}}{r_{ij}^{6}} + 332 q_i \sum_{j=1}^{\text{IRK}} \frac{q_j}{D r_{ij}} \right). \quad (1)$$

Each term is a double sum over the peptide atoms i and IRK atoms j. A and B are van der Waals repulsion and attraction parameters, respectively. r_{ij} is the distance in Å between atoms i and j. q_i and q_j are the point charges on atoms i and j. Equation 1 does not contain an explicit hydrogen-bonding term. We assume that hydrogen bond energies can largely be accounted for in the electrostatic term. A 10-Å cutoff and a dielectric function of $D = 4r_{ij}$ were used. Simulations of docking between IRK and the peptides were executed using the anchor and grow procedure[27] in DOCK.

Docking simulations—AMBER Scoring Function

The results obtained from simulations using the GRID scoring function were further estimated by the AMBER scoring function, in which both the peptides and the interactive site of IRK can be flexible, allowing small structural rearrangements to reproduce the induced-fit while performing the scoring function. In AMBER scoring, the program performs minimization and molecular dynamics (MD) simulation on the peptide, IRK, and the complex individually, and calculates the score as follows:

$$\text{Score } (E_{\text{binding}}) = E_{\text{complex}} - (E_{\text{IRK}} + E_{\text{peptide}}). \quad (2)$$

Where, E is a sum of AMBER MM potentials and solvation free energy derived from the generalized Born/surface area continuum model.[28] The atoms of IRK within 10 Å from the peptide were flexible. A modified GB (OBC) model[29] was used as the generalized Born model. Following 1000 minimization steps, 3000 MD steps (3 psec) were performed at a constant temperature of 310 K. The structures of the complex of the peptide and IRK having the most stable score were figured using PyMOL.

RESULTS

Autophosphorylation of IR in the presence of synthetic peptides in vitro

We investigated the effects of synthetic peptides on the autophosphorylation of IR. The results at 20 μM ATP are shown in Figure 1, where the insulin-stimulated responses of IR without peptides at 10 min were taken as the control and considered to be 100%. DIYET and DYYRK inhibited the autophosphorylation of IR to 20.5 and 40.7% at 4000 μM, respectively (Figures 1a and b, white bars). IC_{50} values of DIYET and DYYRK were 477.8 μM and 1228.8 μM, respectively. In the coexistence of DIYET and DYYRK, the inhibitory effects of these peptides decreased: the mixture inhibited the autophosphorylation of IR to 56.2% at 4000 μM each (Figure 1c). The results concerning the replacement of tyrosine residues in the peptides with alanine (Tyr/Ala), phenylalanine (Tyr/Phe), or phosphotyrosine (Tyr/pTyr) are shown in Figure 2, where the insulin-stimulated responses of IR without peptides at 10 min were taken as the control and considered to be 100%. The Tyr/Ala-substituted peptide, DIAET, and the Tyr/Phe-substituted peptides, DIFET and DFFRK, hardly inhibited the autophosphorylation of IR. The inhibitory potency of DAARK was weaker than that of its parent peptide, DYYRK. The inhibitory effects of the peptides, including phosphotyrosine, DIpYET and DpYpYRK (pY: phosphotyrosine), were

much less than those of their parent peptides, DIYET and DYYRK, respectively; however, the inhibitory effect of DIpYET at low concentrations (40–400 μM) was more than that of DIYET.

Effects of replacing negatively charged amino acids with corresponding neutral amino acids in the peptides on inhibitory potencies

Figure 3 shows the effects of modified peptides in which aspartate and glutamate are replaced with asparagine (Asp/Asn) and glutamine (Glu/Gln), respectively, on the autophosphorylation of IR. The insulin-stimulated responses of IR without peptides at 10 min were taken as the control and considered to be 100%. The maximal concentration of NIYQT was 1000 μM because 4000 μM NIYQT was not completely dissolved. The inhibitory potencies of NIYQT and NYYRK at 20 μM ATP were greater than those of the parent peptides (Figures 3a and b, white bars). IC_{50} values of NIYQT and NYYRK were 24.6 μM and 465.2 μM, respectively.

Effects of the concentration of ATP on the inhibitory potencies of the peptides

We examined the effects of the ATP concentration on the inhibitory potencies of the peptides. IR was incubated with the peptides at various concentrations of ATP (20 μM, 200 μM, and 2000 μM). DIYET and DYYRK were not affected by the concentration of ATP (Figures 1a and b). In contrast, the inhibitory effects of NIYQT and NYYRK significantly decreased as the concentration of ATP increased (Figure 3), indicating that these peptides are ATP-competitive inhibitors.

Effects of the inhibitory peptides on the autophosphorylation of EGFR

In order to evaluate the selectivity of inhibitory peptides for IR, their effects on the autophosphorylation of epidermal growth factor receptor (EGFR), a popular RTK, were estimated (Figure 4). EGF-stimulated responses of EGFR without peptides at 10 min were taken as the control and considered to be 100%. The autophosphorylation of EGFR was significantly inhibited by NIYQT and NYYRK. On the other hand, DIYET hardly inhibited the autophosphorylation of EGFR and the inhibitory effect of DYYRK on EGFR was much less than that on IR.

Detection of phosphorylated peptides by mass spectrometry

In order to investigate whether the peptides are phosphorylated by IR as exogenous substrates, we measured mass spectra of DIYET, DYYRK, NIYQT, and NYYRK after incubation with IR, insulin, and ATP. The results are summarized in Tables I and II. The corresponding ions due to the

phosphorylated peptides were detected for both DIpYET and DpYpYRK in negative-ion operation mode (Table 1 and Figure 5). Phosphorylated NIpYQT was also detected in positive-ion operation mode, while phosphorylated NpYpYRK was not found (Table 2). These results indicate that DIYET, DYYRK, and NIYQT were phosphorylated by IR.

Docking simulations of interactions between inhibitory peptides and the kinase domain of IR

We used DOCK 6 and its accessory programs in order to estimate the binding modes of the modified peptides, NIYQT and NYYRK, and their parent peptides, DIYET and DYYRK. Figure 6 shows schematically the initial position of peptides for docking simulations and the resulting locations of the peptides. Because we expected some inhibitory peptides to bind to the substrate-binding site in the kinase domain of IR (IRK), the initial position of the four peptides was set at the substrate-binding site, which is surrounded by αEF (Pro1178–Asp1183), αG (Asn1215–Met1223), β11 (Leu1170–Leu1171), P+1 loop (Leu1171–Ala1177), and the catalytic loop (His1130–Asn1137).[16]

Fifty conformations of each peptide were obtained from docking simulation using GRID scoring function. They did not converge at a single position (the mean global RMSD value of 50 conformations, DIYET: 9.96 ± 5.20 Å; DYYRK: 7.48 ± 2.56 Å; NIYQT: 7.61 ± 4.21 Å; NYYRK: 6.73 ± 4.43 Å). Figure 7 shows the calculated conformations of DIYET using GRID scoring function. The conformations of the other peptides were similar to Figure 7. Their scores (energy) were also distributed in a large range. We analyzed their scores and estimated occupancy of each conformation according to the Boltzmann distribution. The Boltzmann distribution is expressed as

$$\theta_i = \frac{\exp(-\beta\varepsilon_i)}{\sum_j \exp(-\beta\varepsilon_j)} \qquad \beta = \frac{1}{kT}, \quad (3)$$

where θ is occupancy of a conformation, ε is average energy of a conformation, k is the Boltzmann constant, T is the thermodynamic temperature, and $\Sigma_j \exp(-\beta\varepsilon_j)$ is the partition function. In this case, the GRID score is substituted for ε. We adopted the conformation of each peptide which has the best score (the lowest energy) because their occupancy was nearly 100% except for NIYQT (Table III). The occupancy of NIYQT is 86.3%. Subsequently, the peptides having the adopted conformations and IRK were simulated together using AMBER scoring function to obtain the induced-fit structures.

The simulation showed that the binding sites of the inhibitory peptides are roughly classified into two sites: the ATP-binding region (Site 1) and a region surrounded by αC (Leu1038–Met1051), the Gly-rich loop (Gly1003–Gly1008), and the catalytic loop (Site 2). The ATP-binging region consists of the adenine-binding region (Val1010, Glu1077, Met1079, and Met1139) and the amino acid residues essential to binding the phosphate groups of ATP (Ser1006 and Lys1030). We analyzed hydrogen bonds and salt bridges between the peptides and IRK in the complex having the

most stable score by geometric analysis.[30]

DIYET, the parent peptide, was located at Site 2 and Thr5 was positioned near Asp1132 and Arg1136 in the catalytic loop (Figure 8a), which play a crucial role in phosphate transfer from ATP to the autophosphorylation sites and substrates.[17,31] The Glu4 side chain was within hydrogen-bonding distance for the terminal two nitrogen atoms of the Arg1136 side chain (2.8 Å). These results indicate that DIYET would prevent a substrate from accessing the catalytic loop.

DYYRK, the parent peptide, was located at Site 2, while its N-terminal moiety was located at Site 1 (Figure 8b). The aromatic ring of Tyr2 and Tyr3 covered Asp1132 and Arg1136 in the catalytic loop. The Tyr2 side chain could form a hydrogen bond with the Lys1085 side chain (3.0 Å), which has an important role in substrate binding. These results indicate that DYYRK would inhibit substrate binding to the catalytic loop of IR.

NIYQT was located at Site 1 (Figure 8c). The Thr5 side chain was positioned at the ATP-binding region. The Gln4 backbone and side chain could form hydrogen bonds with the Lys1030 side chain (2.9 Å) and the Arg1136 backbone (2.8 Å), respectively, which play a crucial role in binding the phosphate group of ATP. It is presumed that NIYQT would inhibit the autophosphorylation of IR in an ATP-competitive manner.

While part of the N-terminal moiety of NYYRK is positioned at Site 2, its major part was located at Site 1 (Figure 8d). The aromatic ring of Tyr2 was occupied at the binding site of the ribose ring of ATP. The acetyl group of the peptide could form a hydrogen bond with the Ser1006 backbone (2.9 Å), which is involved in binding the phosphate group of ATP. These results suggest that NYYRK inhibits the autophosphorylation of IR in an ATP-competitive manner.

DISCUSSION

It has been reported that overexpression of IR triggers most human breast cancers.[32] Both ligand-dependent malignant transformation and increased cell growth occur in cultured breast cells overexpressing IR; therefore, inhibitors of IR activity could contribute to the development of a novel anti-cancer drug. In this study, we found that several peptides inhibited the activity of IR. These inhibitory peptides have potential as seed compounds for anti-cancer drugs.

DIYET and DYYRK, which include the amino-acid sequences of the activation loop of IR, inhibited the autophosphorylation of IR (Figure 1). In the coexistence of these peptides, inhibitory potencies decreased. This result indicates that these peptides do not cooperate and would interact with the same region of IR. We presumed that tyrosine residues in the peptides are essential for the inhibitory effects. To characterize the inhibitory effects of the peptides in detail, we replaced tyrosine residues in the peptides with alanine (Tyr/Ala), phenylalanine (Tyr/Phe) or phosphotyrosine (Tyr/pTyr) and investigated the effects of the substituted peptides on the autophosphorylation of IR. Tyr/Ala- and Tyr/Phe-substituted peptides lost their inhibitory potencies (Figure 2), indicating that

tyrosine residues in the peptides play a crucial role in the interaction with IR. The inhibitory effect of DpYpYRK was much weaker than that of its parent peptide, DYYRK (Figure 2), while the inhibitory potency of DIpYET was comparable to that of DIYET. Tyr/pTyr-substituted peptides include amino-acid sequences of the phosphorylated activation loop. In particular, DpYpYRK includes the crucial phosphotyrosine, i.e. pTyr1162, which is predominantly phosphorylated.[33] It is thought that the peptide was repelled from the catalytic loop in the kinase domain like the phosphorylated activation loop. These results suggest that DYYRK behaves as an autoinhibition region, i.e. the activation loop[15–17] despite its short length. On the other hand, DIpYET includes pTyr1158, which is secondarily phosphorylated by IR; therefore, the inhibitory potency of DIEYT was little affected by Tyr/pTyr substitution.

These peptides have amino-acid sequences around the autophosphorylation sites of IR, and we anticipated that the peptides would bind to the substrate-binding site of IR. The most favorable amino-acid sequence of a substrate recognized by IR has been identified.[34] The sequence, XEEEYMMMM (X is an arbitrary amino acid), includes multiple negatively charged amino acids on the N-terminal side of phosphorylatable tyrosine. The negative charges are assumed to be essential to interacting with positively charged amino acids around the substrate-binding site in the kinase domain.[35] On the basis of this assumption, we predicted that the replacement of negatively charged amino acids in inhibitory peptides with uncharged amino acids (i.e., the replacement of aspartate with asparagine (Asp/Asn) or of glutamate with glutamine (Glu/Gln)) would prevent the peptides from binding to IR and reduce the inhibitory effect. Contrary to our prediction, the inhibitory effects of the modified peptides (NIYQT and NYYRK) were greater than those of their parent peptides (Figure 3). A similar observation was found in the previous study on the inhibitory peptides of epidermal growth factor receptor.[36] These results suggest that negatively charged amino-acid residues in the peptides are not involved in the inhibition or that the binding site of NIYQT and NYYRK in IR is different from that of the parent peptides.

In order to investigate this suggestion, we examined the effects of the concentration of ATP on the inhibitory potencies of peptides. While the inhibitory potencies of DIYET and DYYRK were not affected by the concentration of ATP (Figure 1), those of NIYQT and NYYRK were affected (Figure 3). These results indicate that NIYQT and NYYRK are ATP-competitive inhibitors and DIYET and DYYRK are not; therefore, NIYQT and NYYRK are thought to bind to the ATP-binding region in the kinase domain, which is surrounded by non-polar amino acids.[16] NIYQT and NYYRK are less polarized than DIYET and DYYRK. Hence, it is suggested that NIYQT and NYYRK could be accessible to the ATP-binding region. On the other hand, DIYET and DYYRK are not thought to interact with the ATP-binding region. Moreover, the results obtained from mass spectrometry indicate that these peptides are phosphorylated by IR (Table 1 and Figure 5); therefore, DIYET and DYYRK are suggested to behave as a substrate, that is, they would interact with the catalytic loop in the kinase domain, which catalyzes phosphotransfer reactions. In mass spectrometry, it was found that NIYQT is phosphorylated by IR (Table 2) although it is suggested to be an ATP-competitive inhibitor (Figure 3). NIYQT would interact with both the ATP-binging region and the catalytic loop. Hence, NIYQT is expected to inhibit the

autophosphorylation of IR mainly in an ATP-competitive manner and partly in a substrate-competitive manner, and might contribute to the lower IC_{50} value of NIYQT (24.6 μM) more than those of the other peptides.

Non-ATP-competitive inhibitors can more selectively inhibit the activity of target proteins than ATP-competitive inhibitors.[37] Therefore, non-ATP-competitive inhibitory peptides, DIYET and DYYRK, are presumed to inhibit the autophosphorylation of IR selectively. In order to confirm this presumption, we estimated the effects of inhibitory peptides on the autophosphorylation of EGFR, one of the most common RTKs. DIYET hardly inhibited the autophosphorylation of EGFR and the inhibitory effect of DYYRK was less than that on IR (Figure 4). In contrast, the inhibitory effects of NIYQT and NYYRK on the autophosphorylation of EGFR were comparable to that on IR (Figure 4). ATP-competitive inhibitors, NIYQT and NYYRK, had less selectivity for IR, as expected. On the other hand, an inhibitory peptide which is not an ATP-competitive inhibitor, DIYET and DYYRK, would preferentially inhibit the kinase activity of IR rather than that of other RTKs.

We carried out computational simulations in order to obtain more knowledge on the inhibition mechanism. DOCK Suite of Programs 6 was used to estimate interactions between the kinase domain of IR (IRK) and the inhibitory peptides. NIYQT and NYYRK were located on the ATP-binding pocket (Figures 8c and d). This result coincides with the experimental results that NIYQT and NYYRK inhibited the autophosphorylation of IR in an ATP-competitive manner. DIYET and DYYRK were located near the catalytic loop (Figure 8a and b). These results reflect the experimental results that these peptides are not ATP-competitive inhibitors and might interact with the catalytic loop. The docking program has had modest success in predicting which small molecule drugs bind to proteins.[38] The inhibitory peptides appear to be larger than small molecule drugs used in the test cases for DOCK; however, the program predicted that ATP-competitive inhibitors, NIYQT and NYYRK, would bind to the ATP-binding region in IRK, whereas non-ATP-competitive inhibitors, DIYET and DYYRK, would bind to another site (Figure 8). Thus, our results obtained from docking simulations are thought to be reasonable.

Although ATP-competitive inhibitors of tyrosine kinases are popular, substrate-competitive inhibitors have more benefits[37,39] as they are less likely to inhibit other targets because the substrate-binding site is less conserved than the ATP-binding region. Moreover, a substrate-competitive inhibitor does not need to compete with the very high intracellular concentration of ATP (~5000 μM),[40] which leads to the requirement for a high concentration of an ATP-competitive inhibitor for *in vivo* activities.[41] Thus, substrate-competitive inhibitors are suitable for the development of drugs with fewer adverse effects. Indeed, DIYET and DYYRK, which are not ATP-competitive inhibitors, would preferentially inhibit the kinase activity of IR rather than that of EGFR, whereas NIYQT and NYYRK competing with ATP inhibit the autophosphorylation of EGFR (Figure 4).

Although the inhibitory effect of DIYET on the autophosphorylation of IR was reported in our previous study, the inhibition mechanism has not been proved. In this study, we obtained more knowledge about this mechanism. It was found that DIYET is not an ATP-competitive